NASA/TP—2019-220300

# Average Path Profile of Atmospheric Temperature and Humidity Structure Parameters From a Microwave Profiling Radiometer

*Robert M. Manning*
*Glenn Research Center, Cleveland, Ohio*

November 2019

# NASA STI Program . . . in Profile

Since its founding, NASA has been dedicated to the advancement of aeronautics and space science. The NASA Scientific and Technical Information (STI) Program plays a key part in helping NASA maintain this important role.

The NASA STI Program operates under the auspices of the Agency Chief Information Officer. It collects, organizes, provides for archiving, and disseminates NASA's STI. The NASA STI Program provides access to the NASA Technical Report Server—Registered (NTRS Reg) and NASA Technical Report Server—Public (NTRS) thus providing one of the largest collections of aeronautical and space science STI in the world. Results are published in both non-NASA channels and by NASA in the NASA STI Report Series, which includes the following report types:

- TECHNICAL PUBLICATION. Reports of completed research or a major significant phase of research that present the results of NASA programs and include extensive data or theoretical analysis. Includes compilations of significant scientific and technical data and information deemed to be of continuing reference value. NASA counter-part of peer-reviewed formal professional papers, but has less stringent limitations on manuscript length and extent of graphic presentations.

- TECHNICAL MEMORANDUM. Scientific and technical findings that are preliminary or of specialized interest, e.g., "quick-release" reports, working papers, and bibliographies that contain minimal annotation. Does not contain extensive analysis.

- CONTRACTOR REPORT. Scientific and technical findings by NASA-sponsored contractors and grantees.

- CONFERENCE PUBLICATION. Collected papers from scientific and technical conferences, symposia, seminars, or other meetings sponsored or co-sponsored by NASA.

- SPECIAL PUBLICATION. Scientific, technical, or historical information from NASA programs, projects, and missions, often concerned with subjects having substantial public interest.

- TECHNICAL TRANSLATION. English-language translations of foreign scientific and technical material pertinent to NASA's mission.

For more information about the NASA STI program, see the following:

- Access the NASA STI program home page at http://www.sti.nasa.gov

- E-mail your question to help@sti.nasa.gov

- Fax your question to the NASA STI Information Desk at 757-864-6500

- Telephone the NASA STI Information Desk at 757-864-9658

- Write to:
  NASA STI Program
  Mail Stop 148
  NASA Langley Research Center
  Hampton, VA 23681-2199

NASA/TP—2019-220300

# Average Path Profile of Atmospheric Temperature and Humidity Structure Parameters From a Microwave Profiling Radiometer

*Robert M. Manning*
*Glenn Research Center, Cleveland, Ohio*

National Aeronautics and
Space Administration

Glenn Research Center
Cleveland, Ohio 44135

November 2019

## Acknowledgments

The author would like to express his appreciation and thanks to Brian Vyhnalek of NASA for the processing of the radiometer and wind profiling data that was needed to accomplish experimental verification of this technique.



*Level of Review*: This material has been technically reviewed by expert reviewer(s).

Available from

NASA STI Program
Mail Stop 148
NASA Langley Research Center
Hampton, VA 23681-2199

National Technical Information Service
5285 Port Royal Road
Springfield, VA 22161
703-605-6000

This report is available in electronic form at http://www.sti.nasa.gov/ and http://ntrs.nasa.gov/

# Average Path Profile of Atmospheric Temperature and Humidity Structure Parameters From a Microwave Profiling Radiometer

Robert M. Manning
National Aeronautics and Space Administration
Glenn Research Center
Cleveland, Ohio 44135

## Summary

The values of the key atmospheric turbulence parameters (structure constants) for temperature and water vapor, that is, $C_T^2$, and $C_Q^2$, are highly dependent upon the vertical height within the atmosphere thus making it necessary to specify profiles of these values along the atmospheric propagation path. The remote sensing method suggested and described in this work makes use of a rapidly integrating microwave profiling radiometer to capture profiles of temperature and humidity through the atmosphere. The integration times of currently available profiling radiometers are such that they are approaching the temporal intervals over which one can possibly make meaningful assessments of these key atmospheric parameters. These integration times, coupled with the boundary effects of the Earth's surface are, however, unconventional for turbulence characterization; the classical Kolmogorov turbulence theory and related 2/3 law for structure functions prevalent in the inertial subrange are no longer appropriate. An alternative to this classical approach is derived from first principles to account for the nuances of turbulent mechanics met with using radiometer sensing, that is, the large-scale turbulence driven by the various possible boundary conditions within the buoyancy subrange. Analytical expressions connecting the measured structure functions to the corresponding structure parameters are obtained. The theory is then applied to an experimental scenario involving radiometric profile measurements of temperature and shows very good results.

## 1.0 Introduction

The atmospheric turbulence metrics inherent in the definitions of the structure constants of passive additives such as temperature, $C_T^2$, and water vapor (humidity), $C_Q^2$, are not only important in the assessment of the tropospheric turbulence field but also in the assessment of the radio and optical refractive index field in the consideration of the propagation of electromagnetic waves. Temperature and water vapor are the major components that determine the prevailing refractive index field (characterized by the refractive index structure constant, $C_n^2$) and their statistical evaluation is a prerequisite for the performance of image and communications systems that must rely on electromagnetic wave transmission through the atmosphere. Values of these structure parameters are functions of height above the Earth's surface and a comprehensive description of their behavior must include such variation of their values along a vertical path profile through the atmosphere.

Within the confines of classical Kolmogorov turbulence theory, the value of $C_T^2$ can be determined through the operational definition provided by the 2/3 law, that is, $C_T^2 = D_T(d)/d^{2/3}$ where $D_T(d) = \langle (T(r + d) - T(r))^2 \rangle$ is the temperature structure function, the value of which is easily determined through measurement of the temperature difference across the spatial separation $d$ and the subsequent temporal average of its difference is squared. Similarly, the same consideration holds for water vapor. The subject of the present work is the exploratory analysis of a measurement technique that can capture vertical profile values of temperature and water vapor in the atmosphere. In particular, the remote sensing method suggested and described in this work makes use of a rapidly integrating microwave profiling radiometer (Radiometrics Corp. MP–3000A) to capture these profiles. The essence of the method is to capture two such profiles consecutively measured over a time interval of $\Delta t$, the integration time of the radiometer. Then, via the application of the Taylor frozen-flow hypothesis, one forms a single realization of the structure function across the induced spatial separation $\bar{U}\Delta t$, where $\bar{U}$ is a vertical profile of the average wind velocity. Upon ensemble averaging of such measurements, a value of the corresponding structure parameter can be obtained along the vertical profile. The integration time of this particular radiometer is on the order of 30 to 40 s and is such that it approaches the temporal intervals over which one can possibly make meaningful measurements of some key atmospheric parameters. This query, of course, implicitly assumes many things. The major ones are as follows: (1) a relationship similar to the 2/3 law, but applicable to the large-scale turbulence phenomena involved, can be identified and used

to do the actual calculation of the structure function values, (2) applicability of the frozen-flow hypothesis over the integration period $\Delta t$, and (3) the resolution requirements placed upon the radiometer to discern the difference values of temperature and water vapor typical of atmospheric scenarios. The most important aspect of these assumptions is the determination of the relationship that replaces the 2/3 law that only holds under idealistic conditions. That is, one must establish a general function $F(d)$ such that, in the case of temperature, for example, $C_T^2 = D_T(d)/F(d)$ where $d = \bar{U}\Delta t$. The form of this function will be strongly dependent on boundary conditions such as shear flow, buoyancy, stability, $\Delta t$, etc., and of course, should reduce to $F(d) \approx d^{2/3}$ in the Kolmogorov case. The determination of this function will dominate this work as it is key to the entire calculation process that results in the structure parameter values. Also, the frozen-flow hypothesis will be extended to prevail over the relatively large values of $\Delta t$, which too will enter into the determination of $F(d)$ if it is deemed a significant factor.

Section 2.0 begins with a brief review of the theory of the large-scale atmospheric turbulence spatial spectrum near the surface of the Earth. Here, "large-scale" refers to characteristic turbulence sizes on the order of $l \sim \bar{U}\Delta t$; for a nominal horizontal average wind speed of $U \approx 5$ m/s and radiometer integration time of $\Delta t \approx 40$ s, $l \geq 200$ m. Since the radiometer measurements are made at the Earth's surface, it is required to take into account the surface or boundary layer effects on the formation of such large-scale turbulent fluctuations in the presence of the vertical gradients of velocity, temperature, and water vapor within the atmosphere; the well-known Kolmogorov spectrum for the inertial subrange of isotropic turbulent fluctuations cannot be directly applied. Hence, the Kolmogorov theory must be transcended to account for these effects in a generally stratified atmosphere within the buoyancy subrange. Although such phenomena have been considered earlier (Ref. 1), a self-contained theory is given in Section 2.0 that is general enough to quantitatively apply to many turbulence scenarios. Here, stable as well as unstable cases in an atmosphere with vertical gradients of temperature and velocity (shear) are considered. A composite spatial spectrum for both the inertial and buoyancy subranges is then given as a function of atmospheric conditions and the corresponding structure functions for temperature and humidity are derived. The form of the model connecting the structure functions to those determined from the radiometric measurements is then finally derived in Section 3.0, thus determining the function $F(\bar{U}\Delta t)$. Due to the relatively large value for $\Delta t$, a Fourier-Stieltjes treatment is employed, shown in Appendix A, that transcends the usual use of the Taylor frozen-flow hypothesis in the event that it no longer holds in this temporal region. It is established, however, that the hypothesis does hold well for the large turbulent inhomogeneity sizes for which this sensing technique depends. The demands placed on the resolution requirements for temperature and water vapor of the radiometer are then found. Finally, in Section 4.0, experimental demonstration of the remote sensing method will be given.

A preliminary study of this problem was undertaken in Reference 2 where a composite spectrum for the inertial and buoyancy subranges was advanced and used. However, it provided a poor approximation for the desired model of the turbulence scenario. This circumstance is rectified in the present work. Much of the detail of its derivation from first principles is retained here for completeness. It must be noted that many ranges of atmospheric turbulent spectra can be obtained and quantitatively connected to atmospheric parameters from this analysis. This development was necessary to obtain a firm theoretical basis for this type of remote sensing technique.

# 2.0 The Spatial Spectrum of Turbulent Fluctuations in Thermally Stratified Atmosphere With Shear Flow

In this section, expressions for the spatial spectrum of the combined small- and large-scale turbulent flows will be developed and analyzed.

## 2.1 Development of Spectral Model for Atmospheric Turbulence for Large Scales

The incompressible turbulent flow within the atmosphere that governs the spatial and temporal evolution of the velocity field $\bar{V}$ is given by the Navier-Stokes equation; employing the Boussinesq approximation and assuming a constant dynamic viscosity, $\mu$, one has (Ref. 3):

$$\rho_0\left(\frac{\partial V_i}{\partial t} + V_j\frac{\partial V_i}{\partial x_j}\right) = -\frac{\partial P}{\partial x_i} - \rho g_3 + \mu\frac{\partial}{\partial x_j}\left(\frac{\partial V_i}{\partial x_j}\right)$$
$$\frac{\partial V_i}{\partial x_i} = 0, \qquad \bar{V} = V_1\hat{x} + V_2\hat{y} + V_3\hat{z} \tag{1}$$

where $x_i = \bar{x}, \bar{y}, \bar{x}$ for $i$ = 1,2,3, $\rho_0$ and $\rho$ are the mean and instantaneous density, respectively, $P$ is the pressure and $g_3$ is the gravitational acceleration along the vertical $(x_3 \equiv \bar{z})$ axis. Additionally, the atmospheric temperature field $T$, which is the source of density fluctuations, is given by (Ref. 3)

$$\rho_0 c_P \left( \frac{\partial T}{\partial t} + V_i \frac{\partial T}{\partial x_i} \right) = \mu_T \frac{\partial}{\partial x_i} \left( \frac{\partial T}{\partial x_i} \right) \tag{2}$$

where $c_P$ is the heat capacity at constant pressure and $\mu_T$ is the thermal conductivity of air. A similar equation holds for the water vapor field $Q$. In this report, only the temperature field will be considered with the proviso that the final results will hold for $Q$ (so long as $T$ and $Q$ act as passive additives).

Following the detailed procedure given in Reference 4, Equations (1) and (2) are statistically analyzed to give equations involving the Fourier spectra of the velocity and temperature fluctuations:

$$F(k) - \phi_{13}(k) \frac{d\overline{U}}{dz} + \beta \phi_{3T}(k) - 2\nu k^2 \phi(k) = 0 \tag{3}$$

$$F_{TT}(k) - \phi_{3T}(k) \frac{d\overline{T}}{dz} - 2\nu_T k^2 \phi_{TT}(k) = 0 \tag{4}$$

Here, $k$ is the wavenumber, $F(k)$ and $F_{TT}(k)$ are the energy transfer spectra due to the distortion of fluctuation gradients of, respectively, velocity fluctuations and temperature fluctuations, $\phi_{13}(k)$ is the spectrum of the energy due to the work of velocity fluctuations from Reynolds stresses against the mean shear, $\phi_{3T}(k)$ is the spectrum of the energy due to the work of temperature fluctuations transferred by vertical heat flux against the temperature gradient, and $\phi(k)$ and $\phi_{TT}(k)$ are the spectra of, respectively, turbulent energy fluctuations and temperature fluctuations. The mean atmospheric temperature $\overline{T}$ and velocity $\overline{U}$ are, in general, both functions of the height coordinate $z$ within the atmosphere, that is, the atmosphere is stratified. Finally, $\nu \equiv \mu/\rho_0$ is the kinematic viscosity, $\nu_T \equiv \mu_T/(\rho_0 c_P)$ is the thermal diffusivity, and $\beta \equiv g / \overline{T}$ is the buoyancy parameter and $g$ is the gravitational acceleration. Equations (3) and (4) can be integrated to give the more familiar form:

$$\begin{aligned} \varepsilon = {} & 2\nu \int_0^k k'^2 \phi(k')\, dk' - \frac{d\overline{U}}{dz} \int_k^\infty \phi_{13}(k')\, dk' \\ & + \int_k^\infty F(k')\, dk' + \beta \int_k^\infty \phi_{3T}(k')\, dk' \end{aligned} \tag{5}$$

$$\begin{aligned} N = {} & 2\nu_T \int_0^k k'^2 \phi_{TT}(k')\, dk' \\ & - \frac{d\overline{T}}{dz} \int_k^\infty \phi_{3T}(k')\, dk' + \int_k^\infty F_{TT}(k')\, dk' \end{aligned} \tag{6}$$

where the total dissipation of turbulent energy by viscosity is

$$\varepsilon \equiv \int_0^\infty k^2 \phi(k)\, dk \tag{7}$$

and the total dissipation of temperature fluctuations by thermal conductivity is

$$N \equiv 2\nu_T \int_0^\infty k^2 \phi_{TT}(k)\, dk \tag{8}$$

The point of this development is to obtain from Equations (5) and (6) functions for the turbulent velocity spectrum $\phi(k)$ and, most importantly, the temperature fluctuation spectrum $\phi_{TT}(k)$ and associate them to well-defined parameters that characterize the various atmospheric conditions, which can prevail during a radiometer measurement. Once the spectrum $\phi_{TT}(k)$ is obtained, it is a simple matter to calculate the associated temperature (or humidity) structure function and apply it to the radiometer profiles to determine the related parameter, $C_T^2$. However, at this point, the classical problem well known in turbulence theory is met, namely, due to the nonlinearity of the equations obtained (the source of which is the basic nonlinearity of the Navier-Stokes equations), the number of unknowns is larger than the number of equations, that is, a closure problem prevails. Within the spectral approach considered here (as opposed to the statistical correlation approach), further statistical assumptions involving the turbulent energy spectral transfer functions need to be employed, which allow connections of them to $\phi(k)$ and $\phi_{TT}(k)$. This is thoroughly discussed in Reference 4. See also Reference 5 (Sec. 17) for a comprehensive treatment.

The method is essentially as follows. Following Heisenberg's approach (Ref. 6), the $\phi(k)$ given in the third term of Equation (5) is written

$$\int_k^\infty F(k')\, dk' = \eta(k) \int_0^k 2k'^2 \phi(k')\, dk' \tag{9}$$

in which $\eta(k)$ is the kinematic eddy viscosity. For purposes of this development, the expression used for $\eta(k)$ will not be that given in Reference 7 but one that is more appropriate for the large Prandtl numbers (i.e., viscous diffusion exceeding that of thermal diffusion) typical of atmospheric turbulence (Ref. 7):

$$\eta(k) = \gamma \left[ \int_k^\infty \phi(k') k'^{-2}\, dk' \right]^{1/2} \tag{10}$$

where $\gamma$ is a numerical constant on the order of unity. The idea behind the model of Equations (9) and (10) is that the transfer of energy from fluctuations of wavenumbers less than $k$ to fluctuations of wavenumbers larger than $k$ can be taken as occurring through the viscosity that exists between the fluctuation eddies working on the turbulent vorticity formed in the interval 0 to $k$. This viscosity can be modeled as the integral effect of fluctuation eddies with wavenumbers larger than $k$ acting on eddies with wavenumbers less than $k$. The functional form of Equation (10) over that of the one originally recommended by Heisenberg is more appropriate in the case where momentum diffusivity dominates (Ref. 8). Thus, one has from Equations (9) and (10):

$$\int_k^\infty F(k')\,dk' = \gamma\left[\int_k^\infty \phi(k')k'^{-2}\,dk'\right]^{1/2}\int_0^k 2k'^2\phi(k')\,dk' \tag{11}$$

A similar argument can be applied to the last term of Equation (6) allowing one to write (Ref. 4)

$$\int_k^\infty F_{TT}(k')\,dk' = b\gamma\left[\int_k^\infty \phi(k')k'^{-2}\,dk'\right]^{1/2}\int_0^k 2k'^2\phi_{TT}(k')\,dk' \tag{12}$$

where $b$ is the ratio of $\nu_T$ to $\nu$ of the fluctuation eddies; it too is on the order of unity.

The same methodology can be applied to connect the spectra $\phi_{13}(k)$ and $\phi_{3T}(k)$ to $\phi(k)$ and $\phi_{TT}(k)$. To do this, one must account for the interactions between the gradients of the $\bar{U}$ and $\bar{T}$ with the overall turbulent field (Ref. 4). One must also consider the level of interaction that the velocity field has on the temperature gradients within the stratified atmosphere; such interaction concepts were first put forward by Tchen (Ref. 1) (using the term "resonance") who considered the similar problem of deriving a turbulence spectrum perturbed by boundary effects. Here, the case of the strong interaction is considered. For the model of $\eta(k)$ given by Equation (10) and based on these considerations as well as those of the dimensionality of the quantities involved, one has (see Ref. 4 for details)

$$\int_k^\infty \phi_{13}(k')\,dk' = \gamma\left[\int_k^\infty \phi(k')k'^{-2}\,dk'\right]^{1/2}\left[\int_0^k 2k'^2\phi(k')\,dk'\right]^{1/2} \tag{13}$$

and

$$\int_k^\infty \phi_{3T}(k')\,dk' = b\gamma\left[\int_k^\infty \phi(k')k'^{-2}\,dk'\right]^{1/2}\left[\int_0^k 2k'^2\phi_{TT}(k')\,dk'\right]^{1/2} \tag{14}$$

Substituting Equations (11) to (14) into Equations (5) and (6) yields

$$\varepsilon = 2\nu\int_0^k k'^2\phi(k')\,dk' + \eta(k)\left\{\mp\left|\frac{d\bar{U}}{dz}\right|\left[\int_0^k 2k'^2\phi(k')\,dk'\right]^{1/2} + \int_0^k 2k'^2\phi(k')\,dk' + b\beta\left[\int_0^k 2k'^2\phi_{TT}(k')\,dk'\right]^{1/2}\right\} \tag{15}$$

$$N = 2\nu_T\int_0^k k'^2\phi_{TT}(k')\,dk' + b\eta(k)\left\{\mp\left|\frac{d\bar{T}}{dz}\right|\left[\int_0^k 2k'^2\phi_{TT}(k')\,dk'\right]^{1/2} + \int_0^k 2k'^2\phi_{TT}(k')\,dk'\right\} \tag{16}$$

where the upper sign on Equation (15) is for the case $d\bar{U}/dz > 0$ and the lower sign for $d\bar{U}/dz < 0$. Similarly, the upper sign in Equation (16) is for $d\bar{T}/dz > 0$ (which defines the case of stable stratification of the atmosphere) and the lower sign for $d\bar{T}/dz < 0$ (which defines the case of unstable stratification of the atmosphere). Equations (10), (15), and (16) concatenate everything that goes into the determination of the $\phi_{TT}(k)$ spectrum, within the bounds of the assumptions that enter into the closure approximations that allow Equations (11) to (14) to be written. The method of solution for $\phi_{TT}(k)$ using the general model afforded by these relations will be the subject of a future publication. A special case of these equations will be used here to find analytical solutions for $\phi_{TT}(k)$ appropriate for the establishment of analytical connections between the measured temperature (or humidity) structure functions derived from the radiometer output and the structure parameter $C_T^2$ (or $C_Q^2$). To this end, since large-scale turbulence is being considered, one can ignore the contribution of molecular diffusion effects in the evolution of the spectra thus allowing

the first terms on the right sides of Equations (15) and (16) to be dropped. Doing so yields

$$\varepsilon \approx \eta(k)\left\{\mp\left|\frac{d\overline{U}}{dz}\right|\left[\int_0^k 2k'^2\phi(k')dk'\right]^{1/2} + \int_0^k 2k'^2\phi(k')dk' + b\beta\left[\int_0^k 2k'^2\phi_{TT}(k')dk'\right]^{1/2}\right\} \tag{17}$$

$$N \approx b\eta(k)\left\{\mp\left|\frac{d\overline{T}}{dz}\right|\left[\int_0^k 2k'^2\phi_{TT}(k')dk'\right]^{1/2} + \int_0^k 2k'^2\phi_{TT}(k')dk'\right\} \tag{18}$$

Finally, converting to dimensionless variables defined by

$$x = \frac{k}{k_0}, \quad \Phi = \frac{\phi}{\phi_0}, \quad \Phi_{TT} = \frac{\phi_{TT}}{\phi_{TT,0}} \tag{19}$$

$$\Gamma_U = \left|\frac{d\overline{U}}{dz}\right|\left(bN\beta^2\right)^{-1/2}\varepsilon^{1/2} \tag{20}$$

$$\Gamma_T = \left|\frac{d\overline{T}}{dz}\right|(N\beta)^{-1}\varepsilon$$

$$k_0 = \gamma^{1/2}(bN\beta^2)^{3/4}\varepsilon^{-5/4} \tag{21}$$
$$\phi_0 = \gamma^{-3/2}(bN\beta^2)^{-5/4}\varepsilon^{11/4}$$
$$\phi_{TT,0} = \gamma^{-3/2}b^{-9/4}N^{-1/4}\beta^{-5/2}\varepsilon^{7/4}$$

Equations (17) and (18) become

$$K\left(\mp\Gamma_U L^{1/2} + L + M^{1/2}\right) = 1 \tag{22}$$

$$K\left(\mp\Gamma_T M^{1/2} + M\right) = 1 \tag{23}$$

where

$$L = L(x) \equiv \int_0^x 2x'^2\Phi(x')dx' \tag{24}$$

$$M = M(x) \equiv \int_0^x 2x'^2\Phi_{TT}(x')dx' \tag{25}$$

$$K = K(x) \equiv \left[\int_x^\infty x'^{-2}\Phi(x')dx'\right]^{1/2} \tag{26}$$

These equations are written in such a way that allows the use of a solution technique originally suggested by Monin (Ref. 8)—developed further by him in Reference 5 (pp. 225–230 and 417–421)—to obtain analytical approximations to the spectra involved. In particular, from the definitions of Equations (24) and (25), one has

$$\Phi(x) = \frac{1}{2x^2}\frac{dL}{dx}, \quad \Phi_{TT}(x) = \frac{1}{2x^2}\frac{dM}{dx} \tag{27}$$

Equations (22) and (23) can be considered simply as simultaneous algebraic equations to be solved for $L$ and $M$, both as functions of $K(x)$. Then using Equation (27) with these solutions will yield a set of parametric equations involving the spectra as well as the function $K(x)$ along with, of course, the parameters $\Gamma_U$ and $\Gamma_T$ that characterize the atmospheric conditions. Within various combinations of limits of $\Gamma_U$ and $\Gamma_T$, these parametric equations can be first solved for $K(x)$ and then for $\Phi$ and $\Phi_{TT}$ using the additional relation from Equation (26), that is:

$$\frac{dK(x)}{dx} = -\frac{1}{2K(x)x^2}\Phi(x) \tag{28}$$

## 2.2 Solutions of Equations of Spectral Model

Solving Equations (22) and (23) for $L$ and $M$ yield

$$M = F_T \pm \left(F_T^2 - \frac{1}{K^2}\right)^{1/2}, \quad F_T \equiv \frac{1}{K} + \frac{1}{2}\Gamma_T^2 \tag{29}$$

$$L = G + \frac{1}{4}\Gamma_U^2 \pm \Gamma_U G^{1/2}$$
$$G \equiv F + \frac{1}{4}\Gamma_U^2 \tag{30}$$
$$F \equiv \frac{1}{K} + M^{1/2}$$

Differentiating the first relation of Equation (29) with respect to $x$ and using Equation (27) gives, after a bit of manipulation:

$$2x^2\Phi_{TT}(x) = \frac{1}{4K^3x^2}(1 + H_T)\Phi(x) \tag{31}$$

where

$$H_T \equiv 1 \pm (K\Gamma_T^2)^{1/2}\left(1+\frac{K\Gamma_T^2}{4}\right)^{-1/2} \tag{32}$$

Similarly, differentiating the first relation of Equation (30) with respect to $x$ gives, again after some algebraic manipulation:

$$4x^4 = \left[1 \pm \frac{(K\Gamma_U^2)^{1/2}}{2}\left(1+\frac{K\Gamma_U^2}{4} + KM^{1/2}\right)^{-1/2}\right]\frac{1}{K^3}\left(1+\frac{M^{-1/2}}{2}H_T\right) \tag{33}$$

Using these relationships, several combinations and permutations of atmospheric scenarios can be considered. This will form the subject of a future publication. For purposes of this exposition, these equations will now be used to derive analytical expressions for the spectra in two extreme cases:

**(i) $K\Gamma_T^2 << 1, K\Gamma_U^2 << 1$ ; no atmospheric stratification or shear**

Within this approximation, $H_T \approx 1$ and $M \approx K^{-1}$ and Equation (33) significantly reduces to

$$K(x) \approx \left(\frac{1}{4}\right)^{1/3} x^{-4/3} \equiv K_T(x) \tag{34}$$

Using this result in Equation (28) yields the velocity fluctuation spectrum:

$$\Phi(x) \approx \left(\frac{8}{3}\right)\left(\frac{1}{4}\right)^{2/3} x^{-5/3} \equiv \Phi_T(x) \tag{35}$$

which is the result for the inertial subrange that defines this case. Putting this result into Equation (31) then gives for the attendant temperature spectrum:

$$\Phi_{TT}(x) \approx \left(\frac{2}{3}\right)\left(\frac{1}{4}\right)^{-1/3} x^{-5/3} \equiv \Phi_{TT_T}(x) \tag{36}$$

**(ii) $K\Gamma_T^2 >> 1,\ K\Gamma_U^2 >> 1$ ; significant atmospheric stratification and shear**

Here, taking the limits of the relevant expressions becomes a bit more involved but results in $H_T \approx [4/(K\Gamma_T^2)] - 1$ and, once again, $M \approx K^{-1}$. Equation (33) then becomes

$$K(x) \approx \left(\frac{1}{2\Gamma_U^2}\right)^{1/4} x^{-1} \equiv K_U(x) \tag{37}$$

and

$$\Phi(x) \approx 2\left(\frac{1}{2\Gamma_U^2}\right)^{1/2} x^{-1} \equiv \Phi_U(x), \qquad \Phi_{TT}(x) \approx \left(\frac{1}{2\Gamma_U^2}\right)^{-1/2}\left(\frac{1}{\Gamma_T^2}\right)x^{-1} \equiv \Phi_{TT_U}(x) \tag{38}$$

which defines the buoyancy subrange for a stratified atmosphere.

## 2.3 Height-Dependent Spectrum for Both Buoyancy and Inertial Subranges

Thus, the temperature spectrum in the case of no stratification or shear, that is, one which is expected to prevail in the atmosphere away from the surface layer, is, returning to dimensional variables using Equations (19) to (21):

$$\Phi_{TT_T}(k) = Bk^{-5/3}, \qquad B \equiv \left(\frac{2}{3}\right)4^{1/3}\gamma^{-2/3}b^{-1}N\varepsilon^{-1/3} \tag{39}$$

and in the opposite case of shear and stratification, that is, one which is expected to prevail in the atmosphere close to the boundary surface:

$$\Phi_{TT_U}(k) = Ak^{-1}, \qquad A \equiv 2^{1/2}\left|\frac{d\overline{U}}{dz}\right|\left|\frac{d\overline{T}}{dz}\right|^{-2}\gamma^{-1}b^{-2}N^2\varepsilon^{-1} \tag{40}$$

In the general case intermediate to these, one would expect the temperature spectrum to transition from that given by Equation (40) to that given by Equation (39) as one proceeds vertically up through the atmosphere from the Earth's surface to above the boundary layer. Also, Equation (40) will prevail over the large spatial separations between two temperature profiles that are involved with the present radiometer remote sensing technique, that is, over small $k$; Equation (39) governs the spectrum over small spatial separations, that is, large $k$. A composite expression for the temperature spectrum that approaches Equation (39) as $k \to \infty$ and approaches Equation (40) as $k \to 0$ is desired. Unlike the method adopted in Reference 2, the attempted combination of the two turbulence regions considered here begins with the virtual viscosity

functions $K_T(x)$ and $K_U(x)$. Such a combination that reflects the limiting behavior in both the $x$ and $\Gamma_U$ domains defining these particular regions is given by

$$K(x) = \frac{1}{\frac{1}{K_T(x)} + \frac{1}{K_U(x)}} = \frac{\alpha\beta}{\alpha x^{4/3} + \beta x}$$
$$\alpha \equiv \left(\frac{1}{2\Gamma_U^2}\right)^{1/4} \tag{41}$$
$$\beta \equiv \left(\frac{1}{4}\right)^{1/3}$$

(It can be noted that it may be considered too far of a transition to subtend the ranges characterizing no shear to large shear as was done in (i) and (ii) in Section 2.2; intermediate cases may indeed need to be considered in future treatments. The present exposition is only an attempt to find this remote sensing method plausible.) Using this expression in Equation (28) and this intermediate result in Equation (31) yields the composite spectrum of temperature fluctuations:

$$\Phi_{TT}(x) = \left(\frac{1}{4\alpha\beta}\right)(1 + H_T)\frac{\frac{4}{3}\alpha x^{4/3} + \beta}{x^2} \tag{42}$$

This becomes a complicated expression when considering all the ranges of values that $H_T$ can assume for both $dT/dz < 0$ and $dT/dz > 0$, etc. A straightforward but detailed analysis of Equation (42), which will not be reproduced here, yields for cases (i) and (ii):

$$\Phi_{TT}(x) \approx \left(\frac{1}{2\alpha\beta}\right)\frac{\frac{4}{3}\alpha x^{4/3} + \beta}{x^2 + \frac{\alpha\Gamma_T^2}{2}x} \tag{43}$$

where the condition $\Gamma_U^2 > \Gamma_T^2$ must prevail in the limit as $\Gamma_T \to \infty$. Using Equations (19) to (21) and simplifying, Equation (43) finally becomes

$$\Phi_{TT}(k) \approx \left(\frac{B}{k}\right)\frac{k^{1/3} + k_U^{1/3}}{k + k_T} \tag{44}$$
$$(k_U > k_T \text{ as } k_T \to \infty)$$

where two characteristic spatial frequencies appear defined by

$$k_U \equiv \left(\frac{C}{2B}\right)^3 \text{ and } k_T \equiv \frac{C}{2A} \tag{45}$$

with

$$A \equiv 2^{1/2}\left|\frac{d\bar{U}}{dz}\right|\left|\frac{d\bar{T}}{dz}\right|^{-2}\gamma^{-1}b^{-2}N^2\varepsilon^{-1}$$
$$B \equiv \left(\frac{2}{3}\right)4^{1/3}\gamma^{-2/3}b^{-1}N\varepsilon^{-1/3} \tag{46}$$
$$C \equiv 2^{1/4}\left|\frac{d\bar{U}}{dz}\right|^{1/2}\gamma^{-1/2}b^{-1}N\varepsilon^{-1/2}$$

## 2.4 Evaluation of Characteristic Spatial Frequency Coefficients for In Situ Applications via Similarity Theory

Similarity theory can be applied to obtain numerical expressions for the vertical profiles of the coefficient $B$ as well as the prevailing values of $k_U$ and $k_T$ using their relations to the fundamental atmospheric parameters given by Equations (45) and (46). These profile estimates are very helpful (but not required) to use with the corresponding profiles of temperature and water vapor from the radiometer. The basic idea is this: in order to apply the master equation of this remote sensing method, which will be derived below directly from Equation (44), for the specific atmospheric scenarios, the gradient Richardson number $\mathrm{Ri}_g$ can be established from easily measured values of the gradients of temperature $\partial\bar{T}/\partial z$ and wind velocity $\partial\bar{U}/\partial z$ occurring at the surface from which the Monin-Obukhov stability parameter $L$ can be estimated (Ref. 9). Once this has been secured, modified Businger similarity functions and the profile method of Berkowicz and Prahm (Ref. 10) can be employed that yield path profiles for $N$, $\varepsilon$, etc. For example, for $\partial\bar{T}/\partial z = 0.04$ K/m and $\partial\bar{U}/\partial z = 0.09$ (m/s)/m, $\mathrm{Ri}_g = 0.16$ (Pasquill Stability Class F) and $L = 2.96$. Figure 1 displays $\phi_{TT}(k)$ versus $k$ at a height of 200 m.

Similarly, for $\partial\bar{T}/\partial z = -0.03$ K/m and $\partial\bar{U}/\partial z = 0.1$ (m/s)/m, $\mathrm{Ri}_g = -0.098$ (Pasquill Stability Class D) and $L = -25.2$, Figure 2 shows $\phi_{TT}(k)$ versus $k$ at 200 m.

Thus, Equation (44) seems to capture two diverse regions that can prevail in atmospheric turbulence scenarios. It is now finally possible to derive the form of the function $F(d)$ mentioned in the Introduction.

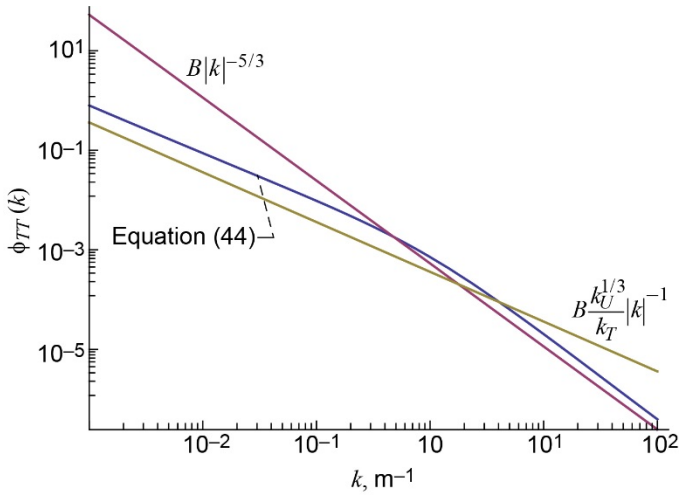


Figure 1.—One-dimensional spatial spectrum $\phi_{TT}(k)$ displaying both buoyancy and inertial subranges for a stable atmosphere at a height of $z$ = 200 m where the Monin-Obukhov stability parameter $L$ = 2.96 and $k_T/k_U$ = 1.02. $k_T$ = characteristic spatial frequency temperature. $k_U$ = characteristic spatial frequency humidity.

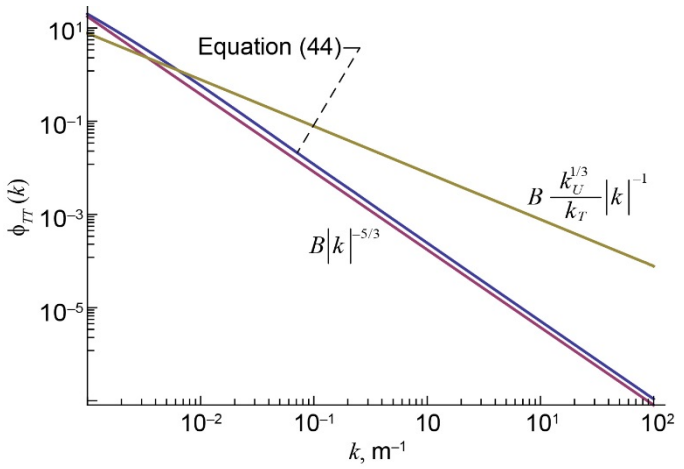


Figure 2.—One-dimensional spatial spectrum $\phi_{TT}(k)$ displaying both buoyancy and inertial subranges for an unstable atmosphere at a height of $z$ = 200 m where the Monin-Obukhov stability parameter $L$ = –25.2 and $k_T/k_U$ = 5.90. $k_T$ = characteristic spatial frequency temperature. $k_U$ = characteristic spatial frequency humidity.

# 3.0 Frozen-Flow Hypothesis and Relating Structure Parameters to Measured Structure Functions—Transcending 2/3 Law

With the spatial spectrum now established that attempts to cover the regions of turbulent activity met within the atmospheric boundary layer in the application of the remote sensing method considered here, it now seems to be a straightforward matter to form the expression for the corresponding structure function (Refs. 5 (Sec. 13) and 11). In the case of a spatial separation $d$ between two spatial points, one has for the temperature structure function:

$$D_T(d) = 2\int_{-\infty}^{\infty}\left(1-\exp\left[-ikd\right]\right)\phi_{TT}(k)\,dk \tag{47}$$

However, in the case of establishing the structure function using measurements separated in time employing the Taylor frozen-flow hypothesis, one usually can write $d = \bar{U}\Delta t$ where $\bar{U}$ is the average atmospheric velocity along the line of length $d$ and obtain

$$D_T(\Delta t) = 2\int_{-\infty}^{\infty}\left(1-\exp\left[-ik\bar{U}\Delta t\right]\right)\phi_{TT}(k)\,dk \tag{48}$$

so long as $\Delta t$ is small enough to assure that the evolution of the turbulent field does not occur. Using the profiling radiometer employs $\Delta t$ ~ 30 to 40 s so the hypothesis of frozen flow may be in question. Appendix A presents a first-principles derivation of the modifications that are induced in the use of Equation (48) over large $\Delta t$ with the result that

$$\begin{aligned} D_T(\Delta t) &= 2\int_{-\infty}^{\infty}\left(1-\exp\left[-ik\bar{U}\Delta t\right]\right)\phi_{TT}(k)\,dk \\ &+\left\langle \upsilon^2\right\rangle \Delta t^2\int_{-\infty}^{\infty}k^2\exp\left[-ik\bar{U}\Delta t\right]\phi_{TT}(k)\,dk \end{aligned} \tag{49}$$

where $\left\langle \upsilon^2\right\rangle << \bar{U}^2$ is the variance of the wind speed fluctuations about $\bar{U}$. In most of the atmospheric applications, $\sqrt{\left\langle \upsilon^2\right\rangle}/\bar{U} \le 0.1$. Equation (49) relates the temperature structure function to the finite time interval over which the samples are formed.

Substituting the spectrum of Equation (44) into Equation (49) and performing the required integrations yield analytical expressions involving combinations of incomplete Γ functions and complex exponentials. Converting these functional combinations into corresponding confluent hypergeometric functions Ψ(*a*;*b*;*z*) for ease of numerical evaluation, one has

$$
\begin{aligned}
D_T(\Delta t) = 4B\Bigg[ & \frac{2}{3}\sqrt{3\pi}\left(\frac{1}{k_t^{2/3}}\right)\left(1-\frac{\mathrm{Re}\left\{\psi\left(\frac{1}{3};\frac{1}{3};-ik_t\overline{U}\Delta t\right)\right\}}{\Gamma\left(\frac{2}{3}\right)}\right) \\
& + \left(\frac{k_U^{1/3}}{k_t}\right)\Big(\mathrm{Re}\left\{\psi\left(1;1;-ik_t\overline{U}\Delta t\right)\right\} \\
& + 0.577 + \log\left(k_t\overline{U}\Delta t\right)\Big) \\
& + \frac{1}{2}\left\langle \upsilon^2\right\rangle \Delta t^2\Bigg( k_t^{4/3}\Gamma\left(\frac{7}{3}\right)\mathrm{Re}\left\{\psi\left(\frac{7}{3};\frac{7}{3};-ik_t\overline{U}\Delta t\right)\right\} \\
& - k_U^{1/3}k_t\,\mathrm{Re}\left\{\psi\left(1;1;-ik_t\overline{U}\Delta t\right)\right\}\Bigg)\Bigg]
\end{aligned}
\tag{50}
$$

To be sure, in the limit:

$$
\begin{aligned}
\lim_{\substack{\Delta t\to 0\\ k_U\to 0}} D_T(\Delta t) &= \frac{4\sqrt{3}B\pi\left(\overline{U}\Delta t\right)^{2/3}}{k_t^{2/3}\Gamma\left(\frac{2}{3}\right)}\mathrm{Re}\left\{(-ik_t)^{2/3}\right\} \\
&= 8.04B\left(\overline{U}\Delta t\right)^{2/3}
\end{aligned}
\tag{51}
$$

which recovers the 2/3 law as well as establishes that the temperature structure parameter $C_T^2$ is identified with $C_T^2 \equiv 8.04B$ which corresponds to the definition of $B$ in Equation (46). However, the second member of Equation (50) that corrects for possible deviations from the frozen-flow hypothesis can be found to be negligible for spatial frequencies $k_t < 1/(\upsilon\Delta t)$; for $\upsilon \sim 0.1\overline{U}$ with $\overline{U} \sim 5$ m/s and $\Delta t$ = 40 s, $k_t < 0.05$ m$^{-1}$. This is the point of demarcation shown in Figure 1 where the spectrum becomes dominated by the effects of the large turbulent inhomogeneity sizes to which this sensing method applies. Hence, one finally establishes the master equation of this proposed remote sensing method:

$$
D_T\left(\overline{U}\Delta t\right) = C_T^2 F\left(\overline{U}\Delta t\right) \tag{52}
$$

where

$$
\begin{aligned}
F\left(\overline{U}\Delta t\right) = \frac{1}{2}\left(\frac{1}{k_t^{2/3}}\right)\Bigg[ & \frac{2}{3}\sqrt{3}\pi\left(1-\frac{\mathrm{Re}\left\{\psi\left(\frac{1}{3};\frac{1}{3};-ik_t\overline{U}\Delta t\right)\right\}}{\Gamma\left(\frac{2}{3}\right)}\right) \\
& + \left(\frac{k_U}{k_t}\right)^{1/3}\Big(\mathrm{Re}\left\{\psi\left(1;1;-ik_t\overline{U}\Delta t\right)\right\} \\
& + 0.577 + \log\left(k_t\overline{U}\Delta t\right)\Big)\Bigg]
\end{aligned}
\tag{53}
$$

Note that in the case of the expression for $F(d)$ mentioned in the Introduction, $d = \overline{U}\Delta t$ since frozen flow approximately holds in this case.

Unlike the situation met with in the earlier version of this theory (Ref. 2), the relative values of the product $k_t\overline{U}\Delta t$ do not allow the use of an asymptotic expansion of Equation (52). However, the functional relationships that enter Equation (52) are easily evaluated along the estimated profiles for $k_t$ and $k_U$. The calculation of the structure function $D_T(\overline{U}\Delta t)$ using consecutive temperature profiles obtained from the radiometer over the period $\Delta t$ can then be transformed to corresponding profiles of $C_T^2$ using Equation (52). Of course, similar considerations and relationships prevail for the case of water vapor and the determination of $C_Q^2$.

The characteristic behavior of $D_T(\overline{U}\Delta t)$ as a function of $\Delta t$ can be obtained from Equation (52). This will now be shown along with simultaneously determining the resolution requirements of the radiometer needed to discern the differences in the temperature structure functions. Consider the case where $\overline{U} = 5$ m/s and take for the numerical value of $C_T^2$ the minimum value observed in atmospheric experiments (Ref. 12), $C_T^2 = C_{T_{\min}}^2 = 0.003$ K$^2$/m$^{2/3}$. Using the same stable atmosphere case employed with the spectrum of Figure 1, the temperature structure function as a function of $\Delta t$ is displayed in Figure 3.

Since this corresponds to a minimum value of $C_T^2$, one can estimate the corresponding minimum value of radiometer temperature resolution through the relation $\Delta T_{\min} \sim \sqrt{D_{T_{\min}}\left(\overline{U}\Delta t\right)}$. Thus, at $\Delta t$ = 40 s, $\Delta T_{\min} \sim 0.11$ K. Correspondingly for $C_Q^2$, $C_{Q_{\min}}^2 = 0.1$ (g/m$^3$)$^2$/m$^{2/3}$ giving $\Delta Q_{\min} \sim \sqrt{D_{Q_{\min}}\left(\overline{U}\Delta t\right)} \sim 0.68$ g/m$^3$. These required resolutions are well above those of most available profiling radiometers.

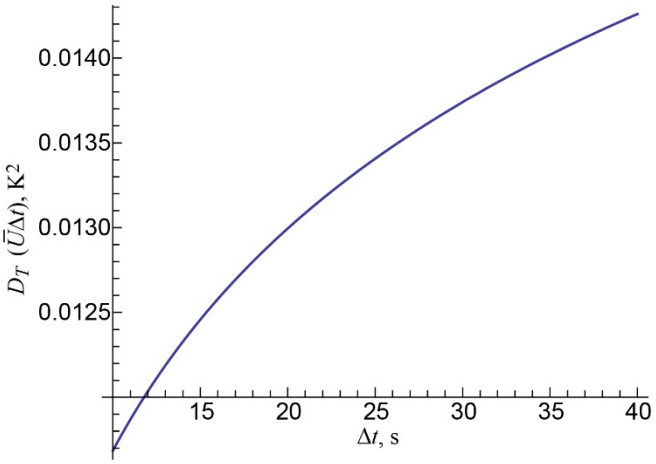


Figure 3.—Temperature structure function as a function of integration time for a stable atmosphere with minimum expected value of temperature structure constant $C_T^2$ at a height of $z$ = 200 m using Equation (52). $C_T^2 = 0.003\ \mathrm{K}^2/\mathrm{m}^{2/3}$. Wind speed fluctuation $\bar{U} = 5.0$ m/s. Monin-Obukhov stability parameter $L$ = 2.96.

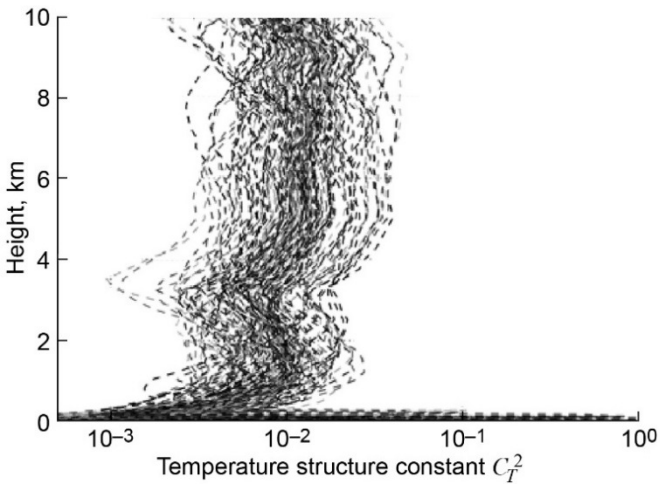


Figure 4.—Calculated vertical profile of temperature structure constant $C_T^2$ from temperature measurements using a Radiometrics Corp. MP–3000A microwave profiling radiometer.

The unstable atmosphere case gives the less stringent resolutions of $\Delta T_{\min} \sim 0.3$ K and $\Delta Q_{\min} \sim 1.8$ g/m$^3$.

## 4.0 Experimental Verification of Remote Sensing Technique

A preliminary experimental demonstration of the method advanced in this report is provided by the use of a profiling radiometer (Radiometrics Corp. MP–3000A) having 35 calibrated channels with a 1.1 s integration time per channel giving $\Delta t \approx 40$ s. The bandwidth per channel is 300 MHz in the 22.0 to 30.0 GHz and 51.0 to 59.0 GHz (K and V) bands. The temperature resolution was 0.1 K. The measurements were taken in January 2013 at the NASA Tracking and Data Relay Satellite System (TDRSS) ground terminal site located at White Sands, New Mexico, with the radiometer pointed to zenith. The dataset comprised 2,100 temperature profiles taken over a 24-h period. The vertical heights of the profiles were discretized over 50 m intervals up to a maximum height of 10 km. Only temperature profiles were considered here. Unfortunately, specific atmospheric conditions during the radiometric data compilation were not available during the time the dataset was obtained. Specific considerations and details of the discretization procedures required as well as application of moving averages to the raw data appear in an earlier publication (Ref. 2). Two major considerations must be noted. First, the need for discrete wind velocity profiles that capture local prevailing conditions can be obtained using available methods (Ref. 13). Second, the required finite integration time of the radiometer restricts the method to apply beginning at a minimum height above the surface. The larger the value of $\Delta t$, the larger the minimum height $h_{\min}$ is above the surface below, which the calculated structure parameters cannot be resolved. Assuming isotropic behavior of the turbulent inhomogenieties that the method can discern, one can simply place this minimum height at the value $h_{\min} = \bar{U}\Delta t$. Of course, contributions of the atmosphere below this height that determine the value of the structure parameters is significant. The experimental derivation of the gradient Richardson number at the radiometer site, as discussed earlier, concurrent with the profile measurements, will secure the surface values and profiles of the structure parameters up to $h_{\min}$.

Figure 4 displays the result of obtaining 143 values of $D_T(\bar{U}\Delta t)$ from the temperature profile dataset and using these derived values in Equation (52) to find 143 corresponding profiles of $C_T^2$. The averaging required to form the structure function values were obtained from 10-min moving averages of the raw differences of adjacent temperature profiles. Since atmospheric measurements were not taken to secure the prevailing values of $k_t$ and $k_U$, nominal constant magnitudes of $k_t = 0.9$ m$^{-1}$ and $k_U/k_t = 1.0$ m$^{-1}$ typical of a stable atmosphere were selected. Wind profiles were created using the method described in Reference 13 in conjunction with historical high-resolution radiosonde data compiled over 3 years at the measurement location. A principle component analysis was then applied to the wind data to obtain a statistical model for $\bar{U}$ as a function of height. (Such a statistical wind profile model

can be obtained using Ref. 13 for any location with a long-term wind profile database.)

Figure 4 shows the minimum height limitation along the abscissa as well as instances where values smaller than $C_{T_{\min}}^2 = 0.003\ \mathrm{K}^2/\mathrm{m}^{2/3}$ are obtained. Unfortunately, no concurrent, independent atmospheric measurements were being made to secure the $C_T^2$ profiles for comparison. However, the morphological behavior of those shown in Figure 4 are the same as those obtained by other methods.

## 5.0 Discussion

The results obtained and displayed in Figure 4 are certainly encouraging enough to provide motivation for a controlled experimental verification of the remote sensing method. To this end, profiling radiometer data for both temperature and water vapor (which was ignored in this report) must be captured. In addition, corresponding simple atmospheric measurements are made to characterize the gradient Richardson number, from which similarity theory can be used, as described in this report, to provide estimates of the profile values of $k_U$ and $k_T$ needed to aid in the use of the master Equation (52) from which $C_T^2$ and $C_Q^2$ profiles can be obtained from the radiometer derived measurements that determine $D_T(\overline{U}\Delta t)$ and $D_Q(\overline{U}\Delta t)$. These atmospheric measurements can also augment other methods used to obtain $C_T^2$ and $C_Q^2$ profile data to provide quasi-independent verification. Also, the use of in situ radiosonde measurements concurrent with the formation of the radiometer data to provide yet another independent verification would be invaluable. Work is now progressing toward these goals.

## 6.0 Conclusions

A remote sensing method using a profiling microwave radiometer to assess vertical path profiles of temperature and water vapor structure parameters has been proposed and experimentally shown to be promising. The ability to accomplish this task relied on two issues: (1) the integration time of profiling radiometers have become small enough for potential consideration of atmospheric turbulent field assessment through the actual measurement of the associated structure functions for the passive additives and (2) the development of a theoretical basis to provide the turbulent fluctuation spectra that is encountered using such unconventionally large measurement times, that is, large-scale turbulence driven by the various possible boundary conditions; one cannot expect Kolmogorov theory to hold that applies only in the inertial subrange. The resulting spectral theory that was obtained seems to have the flexibility to treat many combinations of atmospheric turbulence conditions. Since large-scale phenomena are considered, effects of molecular viscosity are ignored. For purposes of providing a basis for the radiometer remote sensing technique, two disparate regions of atmospheric turbulence activity were chosen, namely, no atmospheric stratification or shear and significant stratification and shear. A composite turbulence spectrum was then obtained from which a general scaling law was derived to replace the specialized 2/3 law. Thus, the structure parameter profiles of $C_T^2$ and $C_Q^2$ (respectively, the constants for temperature and water vapor) can be obtained by forming the structure functions of the respective quantities from the radiometer measurements. The turbulent dynamics theory that was developed also was coupled to similarity theory to provide that capability to perform simple in situ temperature and water vapor gradient measurements to capture the relative magnitudes of the coefficients that appear in the spectrum.

Although the rather quick experimental verification of this technique is promising, more comprehensive verification must be done. Additionally, the use of a composite spectral representation from the theory developed here that employs other atmospheric turbulent conditions intermediate to those used here should also be considered. The issues of just what spectral form to use will be settled through careful atmospheric characterization concurrent with the radiometer measurements.

# Appendix A.— Structure Function Corresponding to Spatial Spectrum Without Use of Frozen-Flow Hypothesis

Consider the atmospheric temperature field $T(t)$ along a vertical path measured by the radiometer at time $t$. After an integration time $\Delta t$, the radiometer measures another temperature field $T(t + \Delta t)$. From these two temporally separated profiles, a temporal temperature structure function can be formed:

$$D_T(\Delta t) = \left\langle \left( T(t+\Delta t) - T(t) \right)^2 \right\rangle \tag{A1}$$

where ⟨---⟩ is the ensemble average which, through ergodicity, is the time average of the indicated function. Hence, several such differential samples must be formed and used to calculate Equation (A1). In terms of the related correlation functions, one can write

$$B_T(\Delta t) \equiv \left\langle T(t) T(t+\Delta t) \right\rangle \tag{A2}$$

and form (Refs. 5 (Sec. 13) and 11) another version of the structure function:

$$D_T(\Delta t) = 2\left[ B_T(0) - B_T(\Delta t) \right] \tag{A3}$$

Now consider the atmosphere containing this temperature field to be translated (convected) by the velocity, $V$, during the radiometer integration period $\Delta t$, and using the slight variation on the very well known prescription by employing the Fourier-Stieltjes transform (Refs. 5 (Sec. 13) and 11) (connecting the temporal statistics of $T(t)$ to the spatial spectrum $\phi_{TT}(k)$ of the spatial statistics governing the temperature field through the spatial coordinate given by $Vt$):

$$\begin{aligned} T(t) &= \int_{-\infty}^{\infty} \exp[ikVt]\, dZ_T(k), \\ \left\langle dZ_T(k)\, dZ_T^*(k') \right\rangle &= \delta(k-k')\, \phi_{TT}(k)\, dk dk' \end{aligned} \tag{A4}$$

in Equation (A2) and substituting this intermediate result into Equation (A3) gives

$$D_T(\Delta t) = 2\int_{-\infty}^{\infty} \left( 1 - \left\langle \exp[-ikV\Delta t] \right\rangle \right) \phi_{TT}(k)\, dk \tag{A5}$$

Unlike the traditional development connecting the structure function to its corresponding spatial spectrum, this more general formulation involves the characteristic function $\langle \exp[-ikV\Delta t] \rangle$ of the velocity field. Following Reference 14, the convective velocity is written as $V = \bar{U} + \upsilon$ where $\bar{U}$ is the average wind speed perpendicular to the vertical coordinate along which the radiometer forms the temperature profile, and $\upsilon$ is its random (fluctuation) component. One then has

$$\left\langle \exp[-ikV\Delta t] \right\rangle = \exp\left[ -ik\bar{U}\Delta t \right] \left\langle \exp[-ik\upsilon\Delta t] \right\rangle \tag{A6}$$

Taking this fluctuating component to be small relative to $\bar{U}$, one can series expand the characteristic function for $\upsilon$ to give

$$\left\langle \exp[-ikV\Delta t] \right\rangle = \exp\left[ -ik\bar{U}\Delta t \right] \left( 1 - \frac{1}{2} k^2 \left\langle \upsilon^2 \right\rangle \Delta t^2 \right) \tag{A7}$$

thus allowing Equation (A5) to be written

$$\begin{aligned} D_T(\Delta t) = {} & 2\int_{-\infty}^{\infty} \left( 1 - \exp\left[ -ik\bar{U}\Delta t \right] \right) \phi_{TT}(k)\, dk \\ & + \left\langle \upsilon^2 \right\rangle \Delta t^2 \int_{-\infty}^{\infty} k^2 \exp\left[ -ik\bar{U}\Delta t \right] \phi_{TT}(k)\, dk \end{aligned} \tag{A8}$$

Equation (A8) gives the relation that is needed to obtain the temperature structure function, measured from the radiometer data, from the combined spectrum of Equation (44). The derivation of this relation transcends the use of the Taylor frozen-flow hypothesis, the use of which may be problematic over the range to time delays $\Delta t$ that prevail for the radiometer integration period. For typical atmospheric situations, one has $\sqrt{\left\langle \upsilon^2 \right\rangle} \Big/ \bar{U} \le 0.1$ over the temporal intervals used here.

## References


1. Tchen, C.M.: On the Spectrum of Energy in Turbulent Shear Flow. J. Res. Natl. Bur. Stand., vol. 50, no. 1, 1953, pp. 51–62.
2. Manning, Robert M.; and Vyhnalek, Brian: A Microwave Radiometric Method to Obtain the Average Path Profile of Atmospheric Temperature and Humidity Structure Parameters and Its Application to Optical Propagation System Assessment. Proc. SPIE 9354, no. 935406, 2015.
3. Monin, Andrei S.; and Yaglom, A.M.: Statistical Fluid Mechanics: Mechanics of Turbulence. Vol. 1, Massachusetts Institute of Technology Press, Cambridge, MA, 1971.
4. Lin, Jung-Tai; Panchev, S.; and Cermak, J.E.: Turbulence Spectra in the Buoyancy Subrange of Thermally Stratified Shear Flows. Project THEMIS Technical Report No. 1, 1969.
5. Monin, Andrei Sergeevich; and Yaglom, A.M.: Statistical Fluid Mechanics: Mechanics of Turbulence. Vol. 2, MIT Press, Cambridge, MA, 1975.
6. Heisenberg, W.: Zur Statistischen Theorie der Turbulenz. Z. Phys., vol. 124, nos. 7–12, 1948, pp. 628–657.
7. Howells, I.D.: An Approximate Equation for the Spectrum of a Conserved Scalar Quantity in a Turbulent Fluid. J. Fluid Mech., vol. 9, no. 1, 1960, pp. 104–106.
8. Monin, A.S.: On the Turbulence Spectrum in a Thermally Stratified Atmosphere. Bull. Acad. Sci. USSR Geophys. Ser., no. 3, 1962, pp. 266–271.
9. Binkowski, F.S.: On the Empirical Relationship Between the Richardson Number and the Monin-Obukhov Stability Parameter. Atmos. Environ., vol. 9, no. 4, 1976, pp. 453–454.
10. Berkowicz, R.; and Prahm, L.P.: Evaluation of the Profile Method for Estimation of Surface Fluxes of Momentum and Heat. Atmos. Environ., vol. 16, no. 12, 1982, pp. 2809–2819.
11. Tatarskii, V.I.: The Effects of the Turbulent Atmosphere on Wave Propagation. U.S. Dept. of Commerce, National Technical Information Service, Springfield, VA, 1971.
12. Humi, Mayer: Estimation of the Atmospheric Structure Constants From Airplane Data. J. Atmos. Ocean. Tech., vol. 21, no. 3, 2004, pp. 495–500.
13. Virtser, A.; Kupershmidt, I.; and Shtemler, Yu. M.: Statistical Model for Meteorological Elements Based on Local Radiosonde Measurements in Mediterranean Region. International Conference on Fluxes and Structures in Fluids, Selected Papers, Moscow, 2005, pp. 350–355.
14. Lumley, J.L.: Interpretation of Time Spectra Measured in High-Intensity Shear Flows. Phys. Fluids, vol. 8, 1965, pp. 1056–1062.